DOI: 10.21062/mft.2025.005 http://www.journalmt.com

Study on Trapped Oil and Cavitation of Jet Fuel Gear Pump

Wei Xu (0009-0009-2877-5338), Xianfeng Zhao (0009-0006-8863-8093), Hongyan Shi (0000-0002-9325-2201), Lijuan Huang (0000-0003-0582-7544)
School of Mechanical Engineering, Guizhou University, Guiyang, China. Corresponding author's E-mail: zxf5111@126.com

In order to explore the causes of trapped oil and cavitation formation during the operation of aviation fuel gear pump to ensure the safe and reliable operation of the pump, dynamic grid technology and Realizable were adopted. The k-ε turbulence model and Schnerr-Sauer cavitation model were used to simulate the three-dimensional transient state of the jet fuel gear pump. The results show that: 1) the air bubbles are mainly distributed in the tooth cavity of the inlet end of the gear pump due to the low inlet pressure and the vortex. 2) Under the effect of high pressure and bubbles at the outlet, an approximately closed tooth cavity is formed near the outlet end, and the trapped oil pressure is generated, whose pressure value is 16 times that of the inlet pressure. 3) As the outlet pressure decreases, the trapped oil pressure in the tooth cavity decreases, but the area of the low pressure area increases, and the cavitation area shows a diffusion trend. 4) The high pressure value formed in the tooth cavity is mainly affected by the speed of the gear. As the speed decreases, the high pressure value gradually decreases to the outlet pressure, and the pressure value decreases slowly with the change of the rotation Angle; The speed decreases, cavitation weakens and the cavitation bubbles formed in the tooth cavity gradually shrink to the oil film between teeth.

Keywords: Gear pump, Fluid simulation, Trapped oil pressure, Cavitation phenomenon, Multiple condition

1 Introduction

Gear pump as one of the most basic hydraulic components, because of its simple structure, reliable operation, low prices advantages, in civil, industrial manufacturing and energy transmission fields have a wide range of applications. However, the trapped oil pressure and the cavitation effect during the operation of the gear pump will cause the gear to be affected by the impact load, resulting in vibration noise, affecting the stable operation of the gear pump and reducing the life of the transmission gear[1, 2].

The phenomenon of trapped oil in gear pump refers to the closed cavity formed between the two pairs of gear teeth meshing at the same time and the two sides of the end plate and the inner surface of the pump shell, which is not communicated with the inlet and outlet oil cavities[3]. Because the size of the closed cavity will change periodically with the rotation of the gear, the working pressure of the oil in the closed cavity will also change dramatically, affecting the stability of the gear pump operation. At present, many scholars have analyzed the variation trend of trapped oil pressure and trapped oil cavity volume of gear pump based on theoretical calculation. GUO et al.[4] found that the volume of the trapped oil chamber between the meshing gear teeth in the involute presents a parabolic change rule, and the trapped oil pressure increases first and then decreases with the change of rotation Angle. When the volume of the trapped oil chamber is the smallest, the trapped oil pressure reaches the maximum value. Sun et al.[5] found that the oil trapping phenomenon can reduce the radial force during oil pressing, but aggravate the radial force during oil suction. CAO et al.[6] found that the greater the number of teeth and modulus, the greater the pressure pulsation in the oil inlet area, the oil trapping area and the oil outlet area. The larger the pressure Angle, the smaller the pressure pulsation in the oil-trapped area, and the smaller the influence on the oil inlet area and the oil outlet area. Although the change trend of trapped oil volume and trapped oil pressure value of gear pump can be obtained based on theoretical calculation, the influence of bubbles generated during gear pump operation is ignored, which deviates from the actual working state of gear pump, thus affecting the accuracy of calculation results.

In the process of gear operation, there is often a violent flow field movement and cavitation bubbles are produced. During the formation and collapse of cavitation bubbles, there will be a severe impact load, which will affect the smooth operation of gear pump and lead to the loss of working pressure of gear pump[7, 8, 9]. In terms of computer software simulation analysis, HONG et al.[10] adopted CFD simula-

tion analysis and found that at high speed, low load, high gear modulus and low viscosity, cavitation phenomenon intensified and extreme pressure fluctuations occurred. Using CFD software, ZAHNG et al.[11] found that cavitation phenomenon and hydraulic oil leakage on both sides of the meshing area were large. In terms of experimental research, ANTONIAK et al.[12] clearly observed the flow process of the internal flow field of gear pump by building a visual experimental platform for the internal flow field of gear pump. DHANANJAY et al.[13] combined numerical simulation with experiments to study the effects of different parameters such as speed and outlet pressure on gear pump performance. FROSINA et al.[14] carried out numerical simulation and experimental analysis of high pressure external gear pump, and predicted the distribution of pressure and cavitation in the chamber of the driving gear and driven gear. ERTURK et al.[15] used the time-resolved particle image velocimeter (TRPIV) to experimentally study the flow field characteristics inside the gear pump to help improve the overall performance of the pump.

To sum up, although a lot of analysis has been carried out on the trapped oil and cavitation phenomenon of gear pump in the existing studies, most of the current articles are based on theoretical calculation to analyze the trapped oil phenomenon of gear pump, while ignoring the influence of cavitation bubbles on the trapped oil phenomenon. In addition, whether there is any correlation between the occurrence of cavitation phenomenon and the occurrence of oil trapping phenomenon has not been clearly explained in the present article. Therefore, this paper analyzes the causes of trapped oil and cavitation during gear pump operation, and analyzes the flow field characteristics of gear pump under different working conditions, providing theoretical reference for ensuring safe and reliable operation of gear pump.

2 Geometric Models and Mathematical models

2.1 Geometric models

The gear pump flow field model simulated in this paper is shown in Figure 1. The gear pump flow field model is divided into three parts: the flow field in the inlet section, the shunt field in the gear section and the flow field in the outlet section. The rotation center of the driving wheel is located at the origin of coordinates (0mm, 0mm, 0mm), the speed is 8214r/min, the rotation direction is counterclockwise, and the inlet pressure of the gear pump is 1.4MPa and the outlet pressure *Po* is 15MPa.The top oil film thickness (the thickness of the oil film formed between the tip of the tooth and the housing) is 0.15mm, and the Oil film thickness between teeth (the thickness of the oil film formed between the two meshing teeth) is 0.125mm.The driving gear and driven gear of the gear pump are straight gear with the same physical parameters, and the relevant physical parameters of the gear are shown in Table 1.The liquid flowing inside is aviation kerosene RP-3, and the related material properties are shown in Table 2.

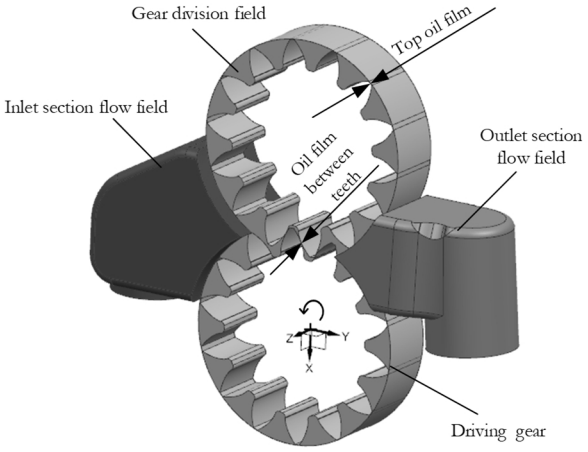

Fig. 1 *Gear pump flow field model*

Tab. 1 *Relevant parameters of gears*

Gear parameters	Value	Unit
Number of teeth *Z*	14	-
Tooth width *B*	22.5	mm
Index circle diameter *d*	66.5	mm
Base circle pitch *Pb*	13.2	mm
Tip radius *Ra*	38	mm
Pitch circle radius *R*	33.25	mm
Pressure Angle α	28	°

Tab. 2 *Material parameter of RP-3*

Material parameter	Value	Unit
Density ρ	800	Kg/m^3
Viscosity μ	0.001184	Pa.s
Thermal conductivity λ	0.13	W/m/K
Specific heat capacity Q	2200	J/Kg/K
Saturated vapor pressure Pv	1329	Pa

2.2 Turbulence model

This paper adopts Realizable k-ε turbulence model, which has good accuracy in the simulation of cavitation turbulence, has been adopted by a large number of scholars [16, 17, 18]. The governing equations of turbulent kinetic energy k and turbulent dissipation rate ε are expressed by equations (1) and (2), respectively:

$$\frac{\partial}{\partial t}(\rho_m k) + \frac{\partial}{\partial x_i}(\rho_m u_i k) = \frac{\partial}{\partial x_j}\left(\left(\mu_m + \frac{\mu_t}{\sigma_k}\right)\frac{\partial k}{\partial x_j}\right) + G_k - \rho_m \varepsilon \tag{1}$$

$$\frac{\partial}{\partial t}(\rho_m \varepsilon) + \frac{\partial}{\partial x_i}(\rho_m u_i \varepsilon) = \frac{\partial}{\partial x_j}\left(\left(\mu_m + \frac{\mu_t}{\sigma_\varepsilon}\right)\frac{\partial \varepsilon}{\partial x_j}\right) + \rho_m C_1 E\varepsilon - \rho_m C_2 \frac{\varepsilon^2}{k + \sqrt{\nu\varepsilon}} \tag{2}$$

$$C_1 = \max\left[0.43\frac{\eta}{\eta + 5}\right] \tag{3}$$

$$\eta = (2\mathrm{E}_{ij} \cdot \mathrm{E}_{ij})^{1/2}\frac{k}{\varepsilon} \tag{4}$$

$$\mathrm{E}_{ij} = \frac{1}{2}\left(\frac{\partial \mu_i}{\partial x_j} + \frac{\partial \mu_j}{\partial x_i}\right) \tag{5}$$

$$\mu_t = \rho_m C_\mu \frac{k^2}{\varepsilon} \tag{6}$$

Where:

G_k…The turbulent kinetic energy generated by the mean velocity gradient,

Σk, σ_ε…The turbulent Prandtl numbers of k and ε, respectively,

k…The turbulent kinetic energy,

ε…The turbulent dissipation rate,

μ_t…The eddy viscosity.

The values of each empirical coefficient in this turbulence model are given by Fluent software by default, C_2=1.9, σ k=1.0, σ_ε=1.2. The accuracy of these values in cavitation simulation has been recognized by other scholars[19,20].

2.3 Cavitation model

The occurrence of cavitation phenomenon is closely related to the saturated vapor pressure of the liquid. When the pressure value in the fluid region is lower than the saturated vapor pressure, the liquid will have cavitation effect; when the pressure value is higher than the saturated vapor pressure, the liquid will condense.

In this paper, Schnerr-Sauer cavitation model is used for simulation. The cavitation model has good stability and is suitable for mixture model and Euler multiphase flow model[19, 20]. In the Schnerr-Sauer cavitation model, when $PV>P$, liquid cavitation occurs, and the equation expression is shown in equation (7). when $PV<P$, liquid condensation, the equation expression is shown in equation (8).

$$R_e = \frac{\rho_v \rho_l}{\rho}\alpha(1-\alpha)\frac{3}{R_B}\sqrt{\frac{2}{3}\frac{P_V - P}{\rho_1}} \tag{7}$$

$$R_c = \frac{\rho_v \rho_l}{\rho} \alpha(1-\alpha) \frac{3}{R_B} \sqrt{\frac{2}{3} \frac{P - P_V}{\rho_1}} \quad (8)$$

$$R_B = \left(\frac{3\alpha}{4\pi n_0 (1-\alpha)}\right)^{1/3} \quad (9)$$

Where:

R_B…The bubble radius [m], its expression is shown in equation (9),

n_0…The number of bubbles per unit liquid volume,

a…The fraction of gas phase volume,

ρ_l…The liquid phase density[kg/m3],

ρ_v…The gas phase density [kg/m3],

ρ…The mixed phase density [kg/m3],

P_V…The saturated steam pressure [Pa],

P…The local pressure [Pa].

3 Grid division and numerical simulation

3.1 Grid division

Because the gear pump runs at a higher speed and the clearance between the meshing and the top of the tooth is smaller, the quality of the mesh is required to be higher. Therefore, different meshes were used for different flow field segments. Tetrahedral meshes were used to divide the flow field in the inlet and outlet areas, and the element size was 2mm.Because the gear flow field area needs to adopt dynamic mesh to simulate the gear movement, the negative mesh volume is easy to be generated in the process of mesh movement, resulting in the failure of calculation. In order to ensure that the gear part has a better mesh quality, 2.5D mesh formed by pulling the triangular prism in one direction is divided, and the element size of the stretching surface is 1mm.At the same time, mesh encryption is carried out on the edge of the gear, and the encryption size is 0.3mm. The final number of grids is 1456220, and the resulting final grid is shown in Figure 2.

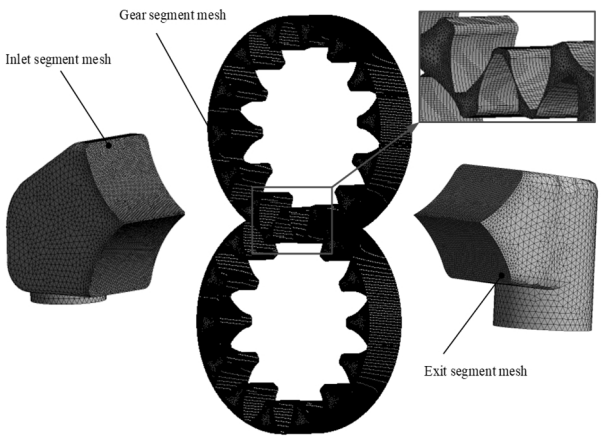

Fig. 2 *Gear pump flow field grid*

3.2 Boundary conditions and simulation Settings

By writing UDF program, dynamic grid technology is used to simulate the rotation process of gear in Fluent software. When setting the cavitation model, mixture of multiphase flow model and Schnerr-Sauer cavitation model are adopted. The saturated vapor pressure is set to 1329Pa and the bubble density is set to 1×10^{11}. Set the inlet as the pressure inlet, the pressure value is 1.4MPa, and the outlet as the pressure outlet, the pressure value is 15MPa. Transient calculation was adopted, the whole cavity was filled with liquid before calculation, and the solution was performed once every 0.1° rotation of the gear, that is, the time step was set to 2×10^{-6}s according to the rotational speed of 8214r/min, and the result of one rotation of the gear was simulated, that is, the end time of the iteration was set to 0.0073s. As shown in Figure 3, in order to describe the simulation results of the gear pump, an observation plane was defined, and the position of the observation plane was the x-y plane of the rotation center of the overdrive wheel, and an observation point (-38mm, 8mm, 78.5mm) was set on the observation plane to observe the pressure variation trend in the tooth cavity.

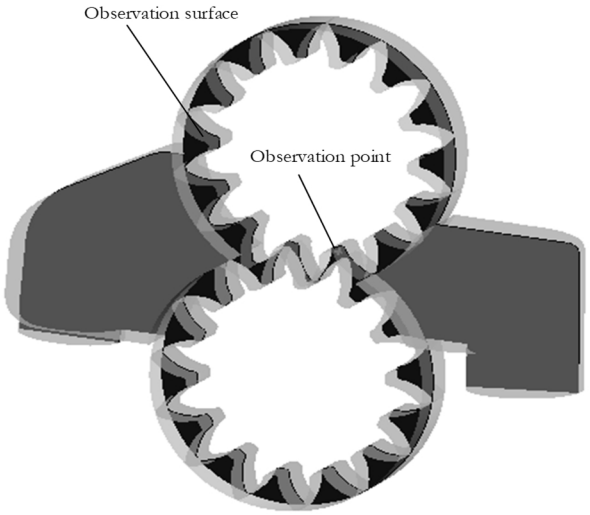

Fig. 3 *Schematic diagram of observation position of simulation results*

4 Calculation results and analysis

4.1 Verification of simulation results

In order to verify the accuracy of the simulation results, this section calculates the outlet theoretical flow of the gear pump and compares it with the simulation results. By calculating the area of the volume swept into the mouth or out of the mouth, the theoretical flow rate of the gear pump is obtained:

$$q = 2\pi B\left(R_a^2 - R^2 - \frac{k_c P_b^2}{12}\right) \quad (10)$$

$$R = mZ \tag{11}$$

$$R_a = \frac{m(Z+2)}{2} \tag{12}$$

$$P_b = \pi m cos\alpha \tag{13}$$

According to Formula (10), the theoretical flow Q (L/min) of the gear pump at different speeds is derived, as shown in Formula (14).

$$Q = 2\pi B\left(R_a^2 - R^2 - \frac{k_c P_b^2}{12}\right)n * 10^{-6} \tag{14}$$

Where:

B…The gear width [mm],

R_a…The radius of the tooth tip of the gear [mm],

P_b…The pitch of the base circle [mm],

R…The pitch circle radius [mm],

m…The gear module [mm],

Z…The number of teeth,

α…The pressure Angle and degree of the gear [°],

k_c…The type coefficient, and the value is 1.02 according to the parameter of the gear pump[21].

n…The speed [r/min].

According to the calculation of the relevant parameters of the gear in Table 1 and Equation (14), the theoretical displacement of the gear pump with 8214r/min is 298.05L/min.

Figure 4 shows the simulated variation curve of gear pump outlet flow Q with rotation Angle θ at 8214r/min. It can be seen from Figure 4 that the pulsation frequency of outlet flow is closely related to the snapping in and snapping out rule of gear, and the average flow rate is 282.04L/min. The flow error between the simulation result and the theoretical calculation is 5.37%, and it is generally believed that the error between the simulation result and the theoretical calculation is less than 10%, indicating that the simulation result is reliable.

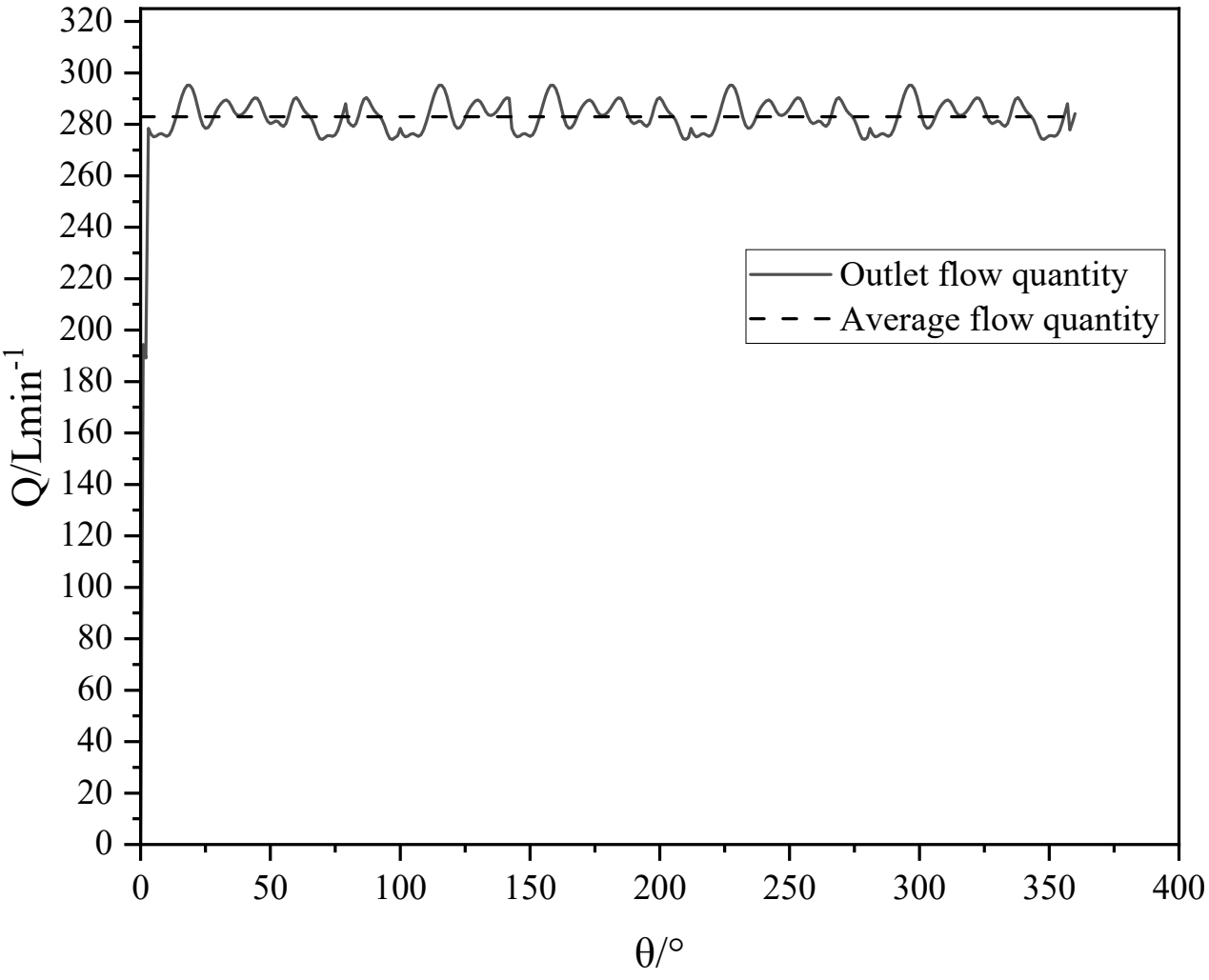

Fig. 4 *Outlet flow curve of gear pump*

4.2 Analysis of gear Pump Cavitation and oil Trapping Phenomenon

4.2.1 Analysis of gear pump Cavitation Formation

Figure 5 is the cloud diagram of steam volume fraction distribution when the gear is turned at different angles θ. It can be seen from Figure 5 that the hydraulic oil in the narrow gap formed at the gear meshing is squeezed by the two meshing gears, resulting in the hydraulic oil flowing into the two sides of the cavity, and the position lacking oil is occupied by the liberated bubbles.

In addition, due to the low pressure in the tooth cavity near the inlet end and the formation of a large number of whirlpool flow in the tooth cavity near the inlet end, a large number of bubbles exist in the tooth cavity near the inlet end. The hydraulic oil at the outlet is compressed by the high pressure at the outlet and the rotation of the gear, and the pressure value is high, and no bubbles are generated. Due to the small gap between the gear and the housing, throttling phenomenon occurs at the position of the tip gap, and the hydraulic oil in the tooth cavity produces a vortex flow driven by the rotating gear, and a large number of bubbles are also produced at this position. As shown in Figure 6, it is also observed that vortices are formed in the tooth cavity and the tip of the tooth, resulting in a large number of bubbles. The positions of the bubbles observed here are highly consistent with the experimental results in literature [12].

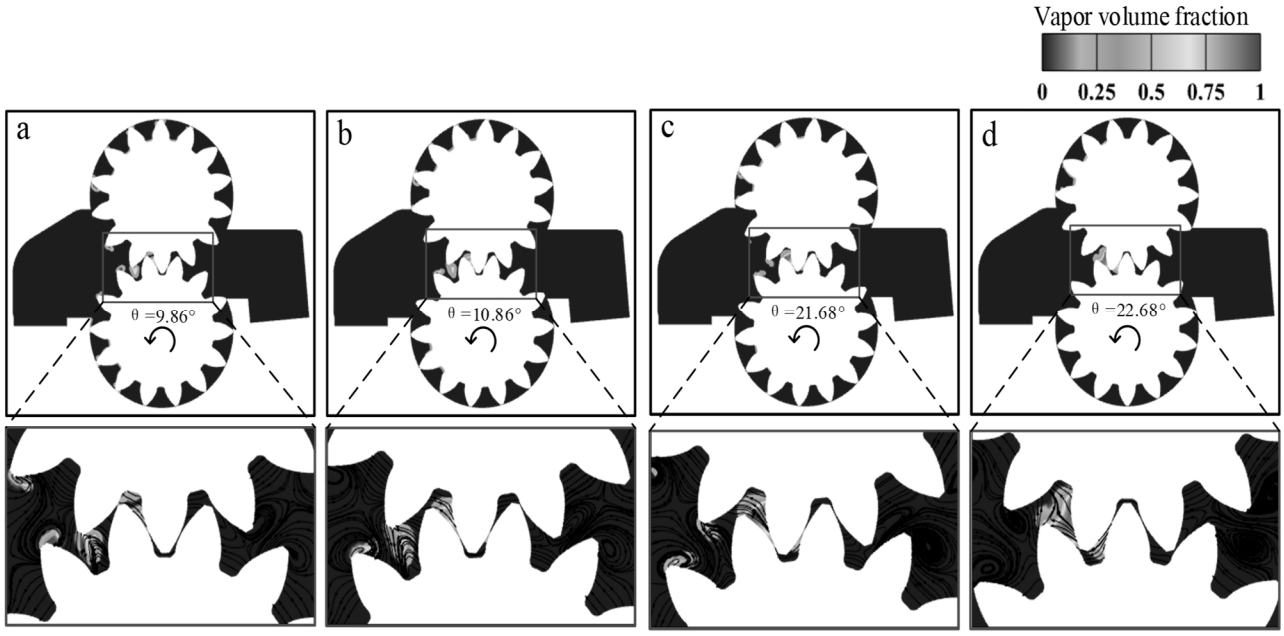

Fig. 5 *Distribution of steam volume fraction at different angles*

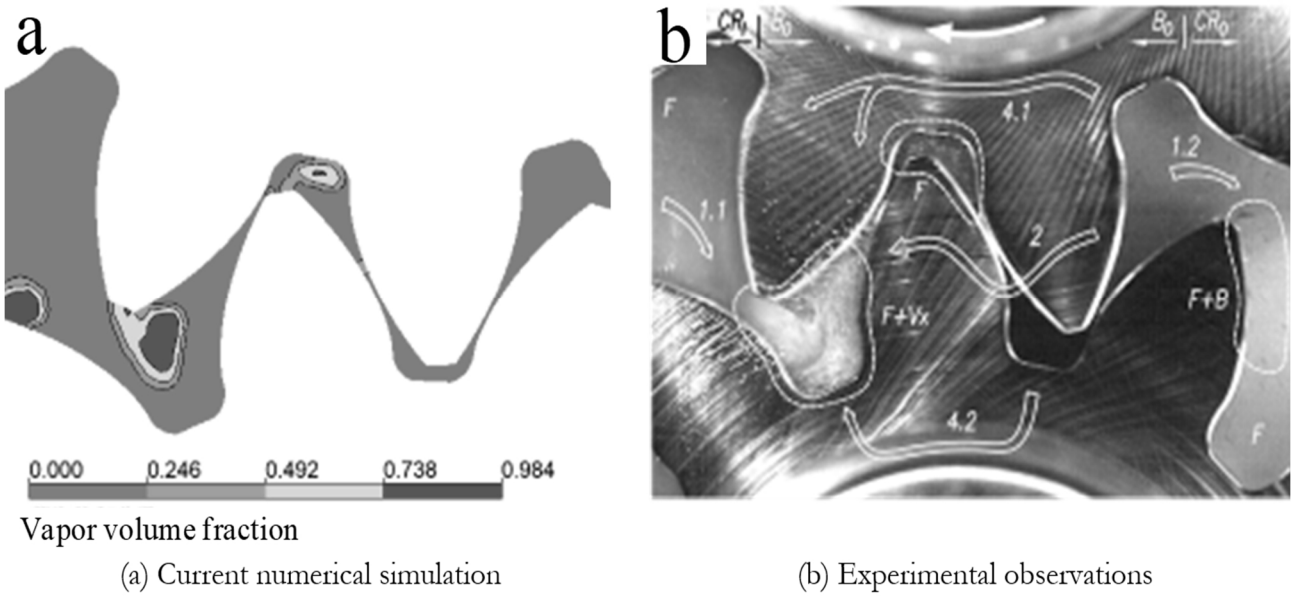

(a) Current numerical simulation (b) Experimental observations

Fig. 6 *Comparison of steam volume fraction distribution*

4.2.2 Analysis of trapped oil pressure formation of gear pump

Figure 7 is the cloud diagram of pressure distribution between teeth when rotating at different angles *θ*. It can be seen from Figure 7 that at the beginning (Figure 7a), hydraulic oil in the narrow gap formed at the gear meshing is squeezed by the two meshing gears, resulting in hydraulic oil flowing into both sides of the cavity and negative pressure forming at the gear meshing gap. At the same time, because the hydraulic oil at the oil film between teeth flows into the cavity at the gear meshing, and the hydraulic oil near the outlet is subject to the effect of high pressure at the outlet, the hydraulic oil is not discharged in time, and bubbles are formed at the oil film between teeth near the inlet end to isolate the flow of hydraulic oil, thus forming an approximately closed cavity at the position of the meshing tooth cavity at the outlet. A higher trapped oil pressure value is generated in its chamber. As the gear rotates 2° Figure 7b), part of the hydraulic oil leaks along the oil film between teeth and the pressure value in the tooth cavity decreases. However, at this time, the gap at the meshing is very small, and most of the hydraulic oil is still trapped in the meshing tooth cavity and is compressed by the rotation of the gear, resulting in the pressure value still higher than the outlet pressure value. When the gear is turned to 21.68° (Figure 7c), the hydraulic oil in the lower part of the tooth cavity at the gear mesh begins to be compressed by the driving gear, and the pressure value in the tooth cavity rises rapidly. With the further rotation of the drive gear (Figure 7d), the hydraulic oil in the tooth cavity is further compressed, and the pressure value in the tooth cavity reaches the maximum value, about 22.77MPa. During the entire operation of the gear pump, the high pressure value formed in the tooth cavity at its engagement is about 16 times the inlet pressure value.

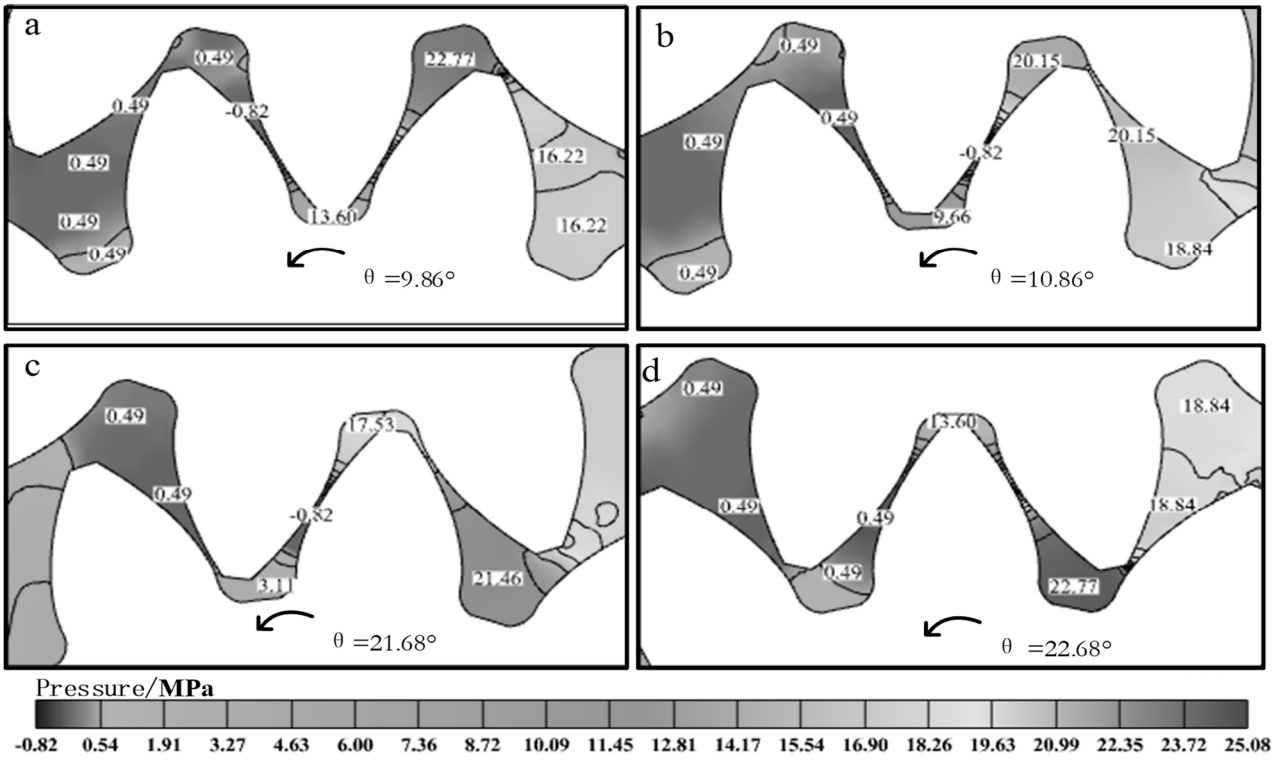

Fig. 7 *Inter-tooth pressure at different angles*

4.3 Analysis of influence of outlet pressure on flow field characteristics of gear pump

This section analyzes the flow field characteristics under the operating conditions of 15MPa, 12MPa, 10MPa, and 8MPa when the rotating speed is 8214r/min.

4.3.1 Pressure distribution analysis under different outlet pressures

Figure 8 shows the pressure distribution cloud diagram under different outlet pressure *Po* conditions when the gear is rotated by 86.74°. As shown in Figure 8, when the outlet pressure *Po* is 15MPa, 12MPa, 10MPa and 8MPa respectively, the pressure value of the oil trapped area in the tooth cavity at the engagement of the gear is 23.23MPa, 19.53MPa, 17.68MPa and 16.70MPa respectively. With the gradual reduction of the outlet pressure, the compression phenomenon generated by the outlet pressure on the tooth cavity is also gradually weakened, and the hydraulic oil is easier to flow out along the slit, and the pressure value in the tooth cavity at the gear mesh is also reduced accordingly.

At the same time, the outlet pressure value decreases, resulting in the reduction of hydraulic oil reflux from the outlet high pressure end to the inlet low pressure end, and the low pressure area in the gear pump shows an increasing trend. When the outlet pressure value reaches 10MPa (Figure 8c), except for the tooth cavity in the oil trap area and a few cavities near the outlet end, most of the tooth cavity of the gear pump shows a low pressure value, and the pressure value is between 1-2MPa. When the outlet pressure value is further reduced to 8MPa (Figure 8d), the pressure value in the tooth cavity of the gear pump is further reduced, and the pressure value in some tooth cavities reaches negative pressure.

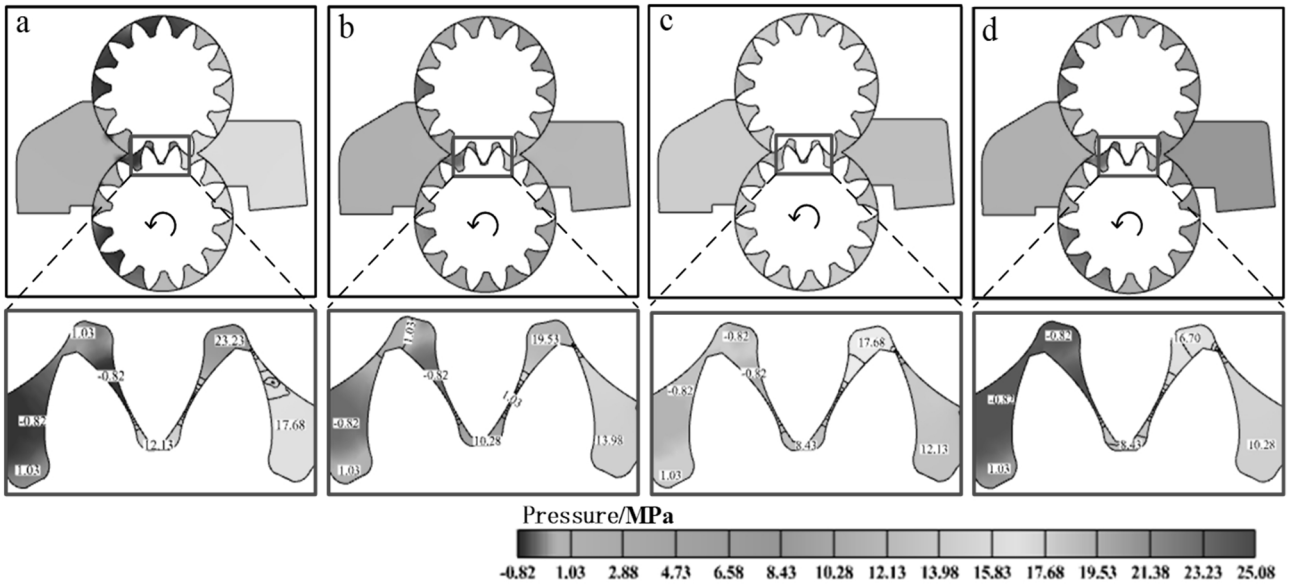

(a) 15MPa; (b) 12MPa; (c) 10MPa; (d) 8MPa

Fig. 8 *Cloud image of pressure distribution under different outlet pressures*

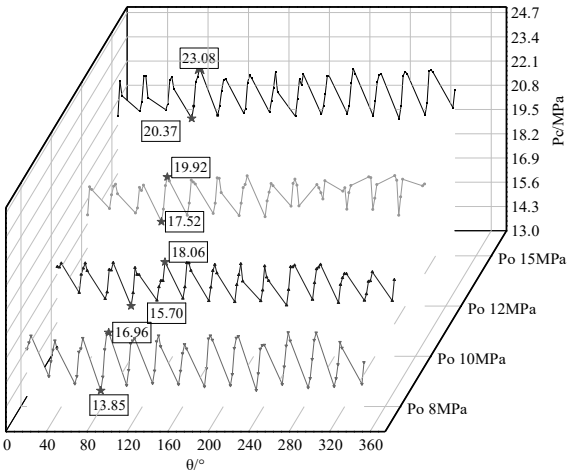

Fig. 9 *Pressure variation curves in the tooth cavity under different outlet pressures*

The variation curve of the pressure value in the tooth cavity *Pc* at the engagement point with the rotation Angle θ under different outlet pressure *Po* conditions at the monitoring point is drawn, as shown in Figure 9. As can be seen from Figure 9, the pressure value in the tooth cavity at the engagement presents a periodic pulsation with the rotation of the gear. With the decrease of the outlet pressure, the trapped oil pressure in the tooth cavity gradually decreases. However, due to the decrease of the outlet pressure value, the compressibility of the hydraulic oil in the tooth cavity in the gear meshing area is weakened, and the pressure change in the tooth cavity is accelerated, which is manifested as the instant increase and decrease of the pressure value. The variation range of the pressure value in the tooth cavity increases with the decrease of the outlet pressure. When the outlet pressure is 15MPa, 12MPa, 10MPa and 8MPa respectively, The variation values of trapped oil pressure in the tooth cavity at gear meshing are 20.37MPa-23.08MPa, 17.52MPa-19.92MPa, 15.70MPa-18.06MPa and 13.85MPa-16.96MPa, respectively.

4.3.2 Analysis of steam volume distribution under different outlet pressures

Figure 10 shows the cloud map of steam volume distribution under different outlet pressure *Po* conditions when the gear is rotated by 86.74°. As shown in Figure 10, the effect of reducing the outlet pressure on the steam volume distribution is not obvious, and a large number of bubbles are stably distributed in the tooth cavities near the inlet and outlet, and there are also a large number of bubbles at the tooth tip of the outlet gear. A small amount of air bubbles are distributed in the slit formed between the top of the tooth and the housing. With the gradual decrease of the outlet pressure, the area occupied by the bubble has a slight diffusion trend.

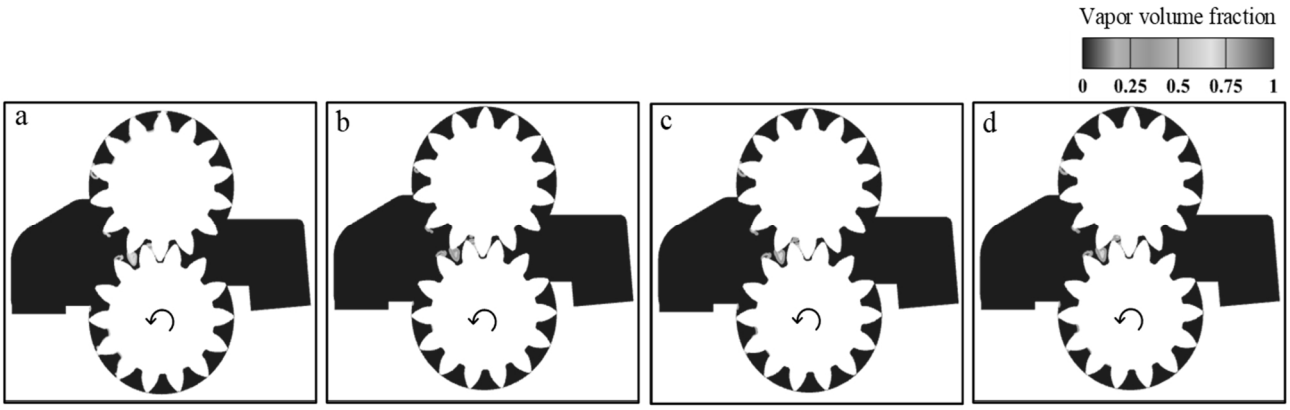

(a) 15MPa; (b) 12MPa; (c) 10MPa; (d) 8MPa

Fig. 10 *Cloud picture of steam volume distribution under different outlet pressures*

Draw the vapor volume percentage η on the observation surface under different outlet pressure *Po* conditions, as shown in Figure 11. As can be seen from Figure 11, although the influence of outlet pressure value on the cavitation of gear pump is not great, and the steam content remains at about 0.65%, the reduction of outlet pressure value leads to the enhancement of the cavitation phenomenon of gear pump. According to Figure 8, the reason for the increase in the proportion of steam volume fraction under the condition of small pressure outlet is that the small pressure outlet increases the area of low pressure value generated in the tooth cavity at the inlet, thus increasing the number of bubble precipitation in the low pressure area, resulting in enhanced cavitation phenomenon.

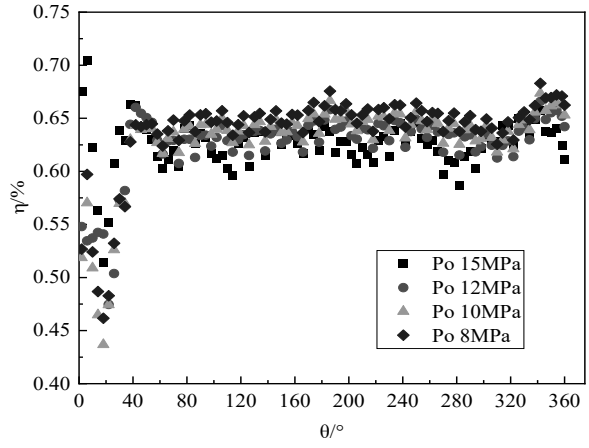

Fig. 11 *Percentage of vapor content on the observation surface at different outlet pressures*

4.4 Influence of Speed on Flow Field Characteristics of gear Pump

In this section, when the outlet pressure is 15MPa, the gear speed is 8214r/min. The flow field characteristics of 6214r/min, 5000r/min and 3000r/min are analyzed.

4.4.1 Pressure distribution analysis at different speed

Figure 12 shows the pressure distribution cloud diagram under different rotating speeds conditions when the gear is rotated by 86.74°. As shown in Figure 12, with the gradual reduction of rotating speed, the instantaneous impact of gear on hydraulic oil is weakened, and the pressure value in the tooth cavity is correspondingly reduced. When the rotating speed is 8214r/min, 6214r/min, 5000r/min and 3000r/min, The pressure values in the tooth cavity at the engagement of the gear are 23.23MPa, 17.68MPa, 15.83MPa and 12.13MPa respectively. At the same time, due to the reduction of rotating speed, the hydraulic oil in the tooth cavity is discharged along the slit for a longer time, and the low pressure area in the tooth cavity is gradually reduced. When the speed reaches 5000r/min (Figure 12c), the low pressure position shrinks to the oil film between teeth of the gear.

The variation curve of the pressure value in the tooth cavity at the engagement of the monitoring point with the rotation Angle under different rotating speeds is drawn, as shown in Figure 13. As can be seen from Figure 13, with the decrease of rotational speed, the high pressure value in the tooth cavity exists for a longer time, and the high pressure value in the tooth cavity gradually decreases to close to the outlet pressure. The above phenomenon shows that the high pressure value generated in the tooth cavity is mainly affected by the high-speed impact of the gear. The higher the speed, the more serious the impact of the gear. The hydraulic oil in the tooth cavity is compressed instantaneously, and the pressure value generated correspondingly increases. At a higher speed, the closed cavity opens instantly, and the high pressure value drops rapidly, while at a lower speed, the high pressure value formed in the cavity is close to the outlet pressure, and under the compression of the outlet pressure, the pressure value in the cavity drops slowly.

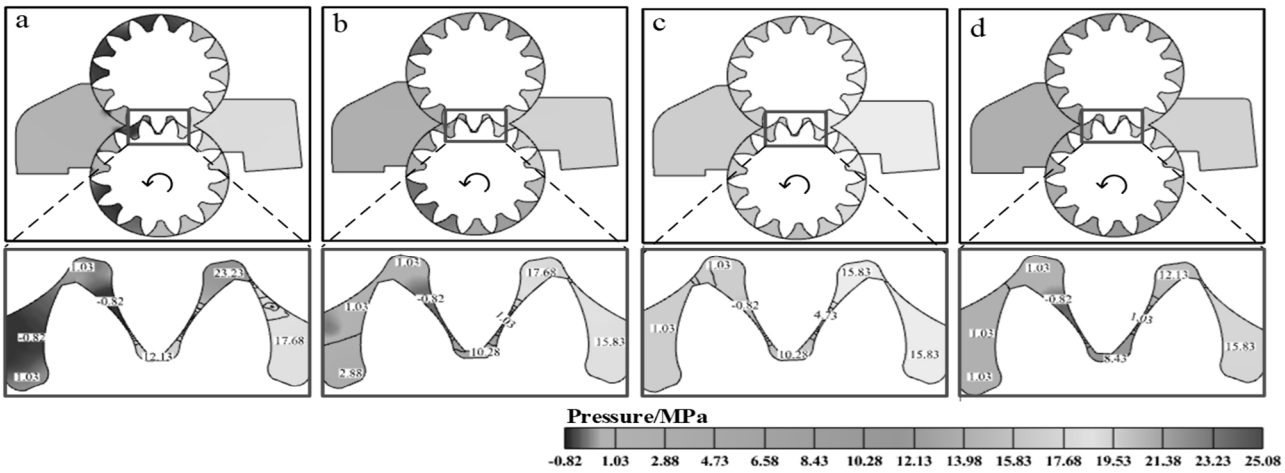

(a) 8214r/min; (b) 6214r/min; (c) 5000r/min; (d) 3000r/min

Fig. 12 *Cloud picture of pressure distribution at different speed*

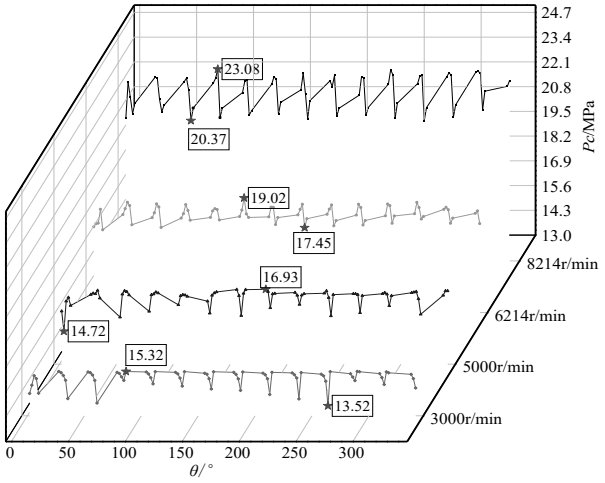

Fig. 13 *Curve of pressure change in tooth cavity at different speed*

4.4.2 Analysis of steam volume distribution at different rotational speeds

Figure 14 shows the cloud map of steam volume distribution under different rotating speed conditions when the gear is rotated by 86.74°.As shown in Figure 14, with the gradual reduction of the rotational speed, the cavitation position gradually decreases and the cavitation formed in the tooth cavity gradually shrinks to the oil film between teeth. The main reason for the above phenomenon is that due to the reduction of speed, the movement characteristics of hydraulic oil are weakened, and the vortex characteristics generated in the tooth cavity are correspondingly weakened, so the cavitation phenomenon is weakened. At 8214r/min, there are bubbles in the top gap of the tooth tip, but when the speed drops to 6214r/min, the bubbles disappear at the top of the tooth tip. It can be seen that the movement characteristics of the flow field at a higher speed are more intense, which is more likely to lead to air separation, thus aggravating the cavitation phenomenon.

The percentage of steam volume on the observation surface under different rotating speed conditions is plotted, as shown in Figure 15. It can be seen from Figure 15 that with the gradual reduction of the rotational speed, the percentage of steam content on the observation surface gradually decreases, and the cavitation weakens. At the higher speed, the number of bubbles produced is more, the bubbles are produced and collapsed more frequently, and the cavitation phenomenon is more intense. Under the condition of low speed, cavitation phenomenon is weak, and the number of bubbles produced under the condition of not turning at the same Angle fluctuates greatly.

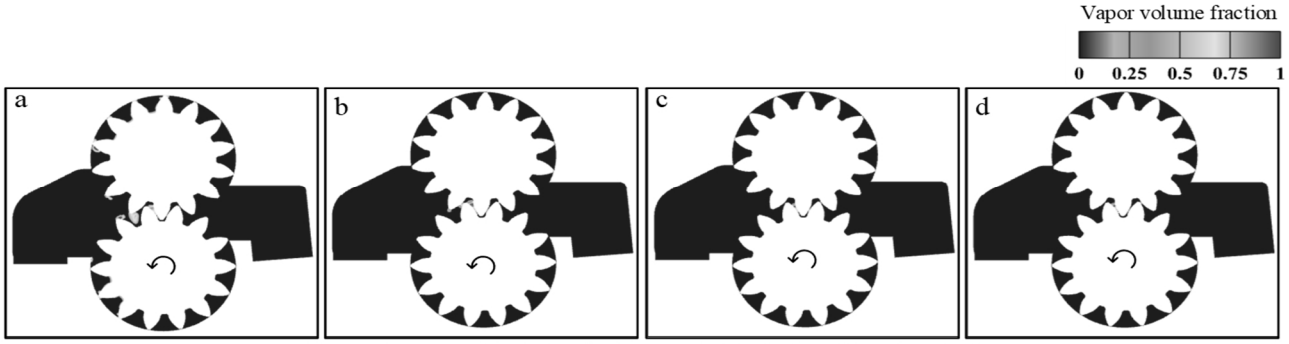

(a) 8214r/min; (b) 6214r/min; (c) 5000r/min; (d) 3000r/min

Fig. 14 *Cloud map of steam volume fraction distribution at different rotational speeds*

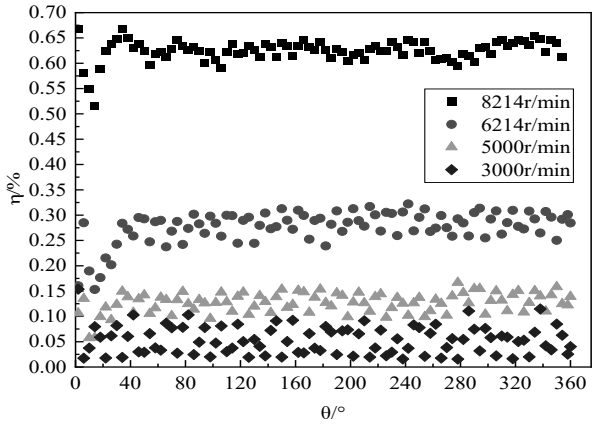

Fig. 15 *Percentage of vapor content on the observation surface at different rotational speeds*

5 Conclusion

- During the operation of the gear pump, bubbles are mainly distributed in the inlet cavity and the oil film between teeth, and the formation of bubbles is related to the vortex and low pressure value generated during the operation of the gear.
- By the outlet high pressure and the formation of bubbles, the gear pump outlet end of the meshing cavity to form an approximately closed cavity, resulting in trapped oil pressure, the generated high pressure value is about 16 times the inlet pressure.
- As the outlet pressure decreases, the compression effect on the oil output end is weakened, the trapped oil pressure in the tooth cavity is reduced, but the area of the low pressure area becomes larger, and the cavitation area shows a small-range diffusion trend.
- The high pressure value formed in the tooth cavity is mainly affected by the speed of the gear. With the reduction of the speed, the high pressure value decreases to close to the outlet pressure, and the pressure value decreases slowly with the change of the rotation Angle. The speed decreases, the cavitation position gradually decreases, and the cavitation bubble formed in the tooth cavity gradually shrinks to the oil film between teeth.

Acknowledgement

This work was financially supported by The Regional Science Foundation of China (No. 52265007).

References

[1] WOO S. Numerical and experimental analysis of vibroacoustic field of external gear pumps. *Purdue University Graduate School*, 2022.

[2] WOO S, VACCA A. An investigation of the vibration modes of an external gear pump through experiments and numerical modeling. *Energies*, 2022, 15: 796.

[3] HE C X. Hydraulic components. *Beijing, China Machine Press*.

[4] GUO S X, GUAN, X F. Simulation research on trapped oil pressure of involute internal gear pump. *Mathematical Problems in Engineering*, 2021: 8834547.

[5] SUN F C, LI Y L, ZHONG F. Research and quantitative analysis of the radial force impacted by trapped-oil pressure in external gear pumps. *Journal of China Agricultural University*, 2018,23 (12): 131-137.

[6] CAO R, LI H C, ZHU J X, et al. Analysis of pressure pulsation in aviation gear pump. *The 11th Asia Conference on Mechanical and Aerospace Engineering ACMAE*, 2020.

[7] MITHUN M G, PHOEVOS K, IOANNIS K K, et al. Numerical simulation of three-phase flow in an external gear pump using immersed boundary approach. *Applied Mathematical Modelling*, 2019, 72: 682-699.

[8] VACCA A, GUIDETTI M. Modelling and experimental validation of external spur gear machines for fluid power applications. *Simul Model Pract Theor*, 2011, 19: 2007–2031.

[9] YOON O, PARK B H, SHIM J, et al. Numerical simulation of three-dimensional external gear pump using immersed solid method. *Applied Thermal Engineering*, 2017, 118: 539-550.

[10] HONG I, ANESHANSLEY E, CHAUDHURY K, et al, Stochastic microcontact model for the prediction of gear mechanical power loss. *Tribology International*, 2023, 183: 108413.

[11] ZHANG X G, LIANG Z. Geometric Modeling and CFD Simulation of curvilinear cylindrical gear pumps. *Iran J Sci Technol Trans Mech Eng*, 2023, 47: 1–17.

[12] ANTONIAK P, STRYCZEK J. Visualization study of the flow processes and phenomena in the external gear pump. *Archiv Civ Mech Eng*, 2018, 18: 1103–1115.

[13] DHANANJAY G A, NIHAL D D, MOHAN P K. Experimentation and 2D fluid flow simulation over an external gear pump, *Phys: Conf Ser*, 2023, 2601: 012029.

[14] FROSINA E, SENATORE A, RIGOSI M. Study of a High-Pressure External Gear Pump with a Computational Fluid Dynamic Modeling Approach. *Energies*, 2017, 10(8): 1113.

[15] ERTURK N, VERNET A, CASTILLA R, et al. Experimental analysis of the flow dynamics in the suction chamber of an external gear pump. *Int J Mech Sci*, 2011, 53: 135–144.

[16] ZHU J K, WANG S H, ZHANG X B. Influences of thermal effects on cavitation dynamics in liquid nitrogen through venturi tube. *Physics of Fluids*, 2020, 32 (1): 012105.

[17] STANISLAV J, KAREL F. Pressure Analysis on the Surface Gearing Investigated by Numerical Simulation of Oil Flow in the Tooth Wheel Gap. *Manufacturing Technology*, 2015, 11(01).

[18] BLANKA S, JAN S. Simulation of Liquid Flow in Pipe. *Manufacturing Technology*, 2013, 12(01).

[19] SCHNERR G H, SAUER J. Physical and numerical modeling of unsteady cavitation dynamics. *4th International Conference on Multiphase Flow (ICMF-2001), New Orleans, USA, May 27-June 1*, 2001.

[20] OLEKSANDR P, ANDRIY Z, JAN K, et al. Calculation of the Characteristics of the Multigap Seal of the Centrifugal Pump, in Dependence on the Chambers' Sizes. *Manufacturing Technology,* 2020, 09(07).

[21] LIU P，LI Y L，SONG A R. An innovation calculation method for theoretical flow of gear-pumps with different backlash value and relief groove layout[J]. *Fluid Machinery*, 2024, 52(01): 69-75.